

APPENDIX H

Geostatistical Analyses

TENNESSEE VALLEY AUTHORITY
Energy Research & Technology Applications
Environmental and Engineering Services
Special Projects

Mapping of Soil Lead at the Twin Cities Phytoremediation Site

WR99-2-520-207

Prepared by
Hank Julian, P.E., P.G.

Engineering Laboratory
Norris Tennessee

October 1999



Mapping of Soil Lead at the Twin Cities Phytoremediation Site

1.0 Introduction

During phytoremediation studies at Sites C and 129-3, soil samples were manually collected from shallow soil horizons and analyzed for total lead. The spatial locations of all samples are based on 90- x 90-ft sampling grids subdivided into 36 cells with dimensions of 15 x 15 feet. Generally, soil samples were obtained at two depths, both before and after remedial crop amendments, at a respective site (as follows).

<u>Sampling Event</u>	<u>Sample Intervals (inches)</u>
Initial	0 to 6 and 6 to 12
Pre-Corn Amendment	0 to 12 and 12 to 24
Post-Corn Amendment	0 to 12 and 12 to 24
Pre-Mustard Amendment	0 to 12 and 12 to 24
Post-Mustard Amendment	0 to 12 and 12 to 24

In order to examine the spatial characteristics of soil lead sampling results at the site, comparative mapping of two sampling events has been conducted using exact and smoothing interpolation techniques. For the purposes of this analysis, only initial and post-mustard amendment sampling results are considered. As the names imply, the initial sampling event was conducted prior to any remedial work at the site; whereas, post-mustard soil samples were collected subsequent to the last site remedial amendment.

2.0 Methods

For this analysis, the commercial software package, Surfer (Golden Software, Inc., 1999), was used in developing two-dimensional plots of interpolated soil lead data. The exact interpolation technique used for generating soil lead maps is triangulation with linear interpolation based on optimal Delaunay triangulation. Lee and Schachter (1980) present a complete discussion of (Delaunay) triangulation, including the details of two algorithms and the underlying mathematical proofs. Lawson (1977) is equally informative. The algorithm presented in Guibas and Stolfi (1985) form the basis for this implementation. Triangulation with linear interpolation works best when data are evenly distributed over the grid area. Data sets that contain sparse areas result in distinct triangular facets on the resultant map. Exact interpolators honor data points exactly when the point coincides with the grid node being interpolated. In other words,

a coincident point carries a weight of essentially 1.0 and all other data points carry a weight of essentially zero.

The smoothing interpolation technique used in developing corresponding soil lead maps is point kriging based on a two-dimensional algorithm contained in Abramowitz and Stegun (1972). Kriging is a geostatistical gridding method that has proven useful and popular in many fields. This method produces visually appealing maps from irregularly spaced data. Kriging attempts to express spatial trends suggested in data, so that, for example, high values might be interconnected rather than isolated by “bull's-eye” type contours. For a detailed derivation and discussion of kriging, see Journel and Huijbregts (1978) or Cressie (1991). In this analysis, the krigged grid is custom-fit to a given data set by specifying an appropriate variogram model (a measure of how quickly things change on the average). The underlying principle is that, on the average, two observations closer together are more similar than two observations farther apart. Because the underlying processes of the data often have preferred orientations, values may change more quickly in one direction than another. As such, the variogram is a function of direction. The variogram model mathematically specifies the spatial variability of the data set and the resulting grid file. The interpolation weights, which are applied to data points during the grid node calculations, are direct functions of the variogram model.

3.0 Data Analysis

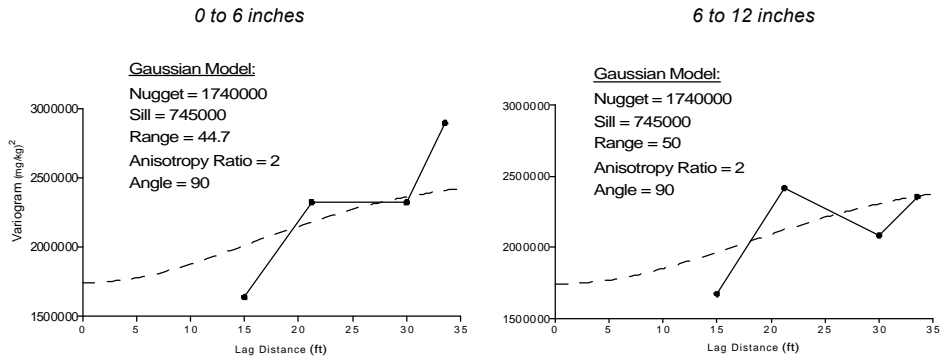
Table 1 presents summary statistics of total lead in soil at Site C from initial and post-mustard sampling events. As shown, although samples were obtained from every cell (36 each) before remediation began at the site, only 22 samples could be collected following the mustard crop amendment. The standard deviations and variance values associated with each sampling event are very high.

Table 1
Summary Statistics of Total Lead in Soil (mg/kg) at Site C
From Initial and Post-Mustard Sampling Events

Sampling Event	Sample Interval (inches)	Number of Samples	Minimum	Median	Maximum	Average	Standard Deviation	Variance
Initial	0 to 6	36	1240	2360	8170	2615	1318	1.74E+06
Initial	6 to 12	36	1050	2570	7150	2851	1319	1.74E+06
Post-Mustard	0 to 12	22	659	1610	10300	2317	2236	5.00E+06
Post-Mustard	12 to 24	22	428	3190	10300	3862	2889	8.34E+06

Figure 1 shows variograms developed for Site C soil sampling results. Variograms for the initial lead sampling event (by depth interval) were fit using similar Gaussian models. The nugget effect of both initial lead variograms (Figure 1a) is high (1,740,000 [mg/kg]²). In the case of all variograms generated for this study, the nugget effect represents error variance, a measure of the direct repeatability of the data measurements. The specified nugget effect causes kriging to become more of a smoothing interpolator, implying less confidence in individual data points versus the overall trend of the data (i.e., the higher the nugget effect, the smoother the resulting grid). Variogram models (Figure 1b) for post-mustard sampling intervals are Gaussian and linear curves for the shallow (0 to 12 inches) and deeper (12 to 24 inches) soil horizons, respectively. As in the case of the initial lead variograms, post-mustard variograms exhibit large nugget effects (3,000,000 [mg/kg]²).

(a) Initial Lead



(b) Post-Mustard

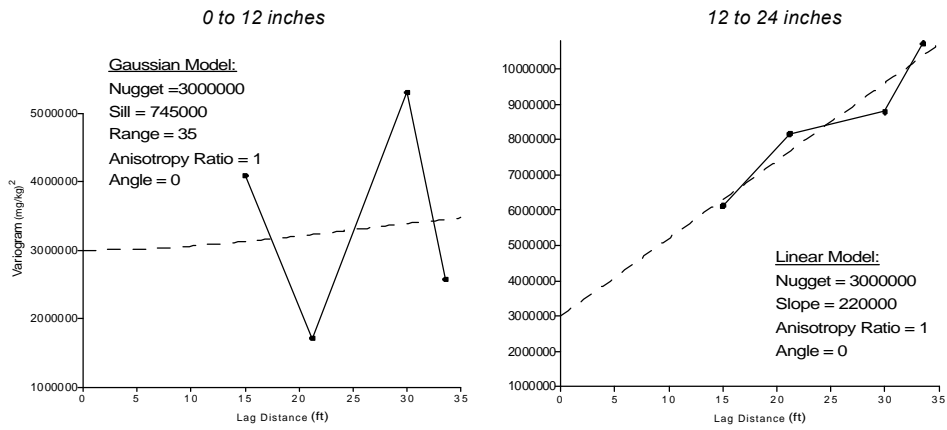


Figure 1
Variograms of Site C Analytical Data from
(a) Initial Soil Lead Sampling and (b) Post-Mustard Amendment Soil Lead Sampling

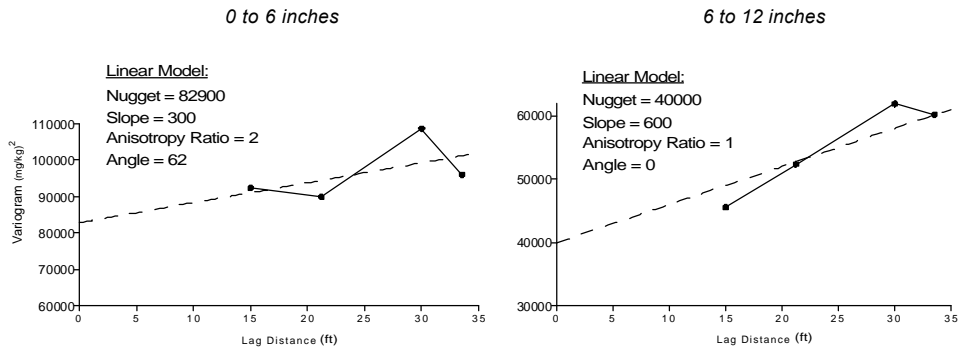
Table 2 presents summary statistics of total lead in soil at Site 129-3 from initial and post-mustard sampling events. As shown, samples were obtained from every cell (36 each) at the site for all sampling events. As at Site C, the standard deviations and variance values associated with each sampling event at Site 129-3 are very high.

Table 2
Summary Statistics of Total Lead in Soil (mg/kg) at Site 129-3
From Initial and Post-Mustard Sampling Events

Sampling Event	Sample Interval (Inches)	Number of Samples	Minimum	Median	Maximum	Average	Standard Deviation	Variance
Initial	0 to 6	36	6	188	1730	329	353	1.25E+05
Initial	6 to 12	36	3	218	918	259	237	5.61E+04
Post-Mustard	0 to 12	36	10	62	1382	200	317	1.00E+05
Post-Mustard	12 to 24	36	3	40	669	114	150	2.25E+04

Figure 2 shows variograms developed for Site 129-3 soil sampling results. Variograms for the initial lead sampling event (by depth interval) were fit to a linear model. The nugget effects of both initial lead (Figure 2a) and post-mustard (Figure 2b) variograms are high as found with Site C.

(a) Initial Lead



(b) Post-Mustard

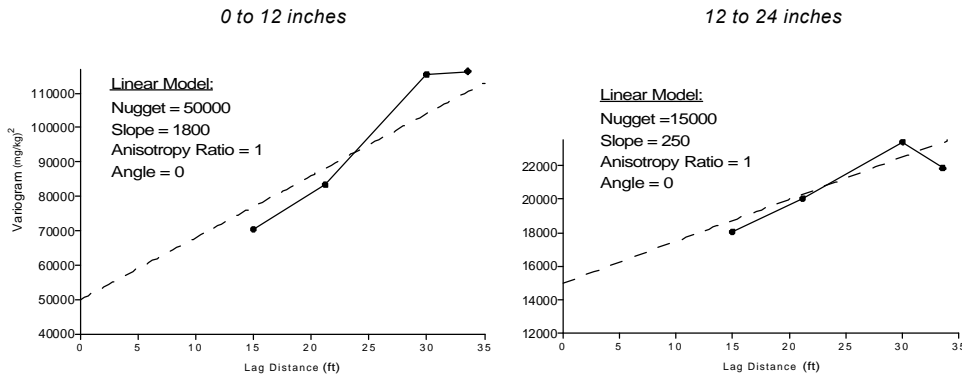


Figure 2
Variograms of Site 129-3 Analytical Data from
(a) Initial Soil Lead Sampling and (b) Post-Mustard Amendment Soil Lead Sampling

4.0 Results and Conclusions

The mapped results of exact and smoothing interpolations of the Site C initial soil lead data are shown in Figures 3a and 3b, respectively, based on depth interval. As shown in Figure 3b, there are no obvious spatial trends in the data. Observations are similar in Figure 4, which displays maps of post-mustard sampling results. There appear to be no obvious trends in the data that can be delineated using geostatistical methods and there is no clear advantage for its application in this particular case. There were high variance values exhibited at both depth intervals.

Other than possible higher soil lead concentrations on the southern side of Site 129-3, no obvious spatial trends are observed in mapped results of soil lead data (Figures 5 and 6). As at Site C, soil sampling results at Site 129-3 exhibit a high degree of variance, regardless of depth.

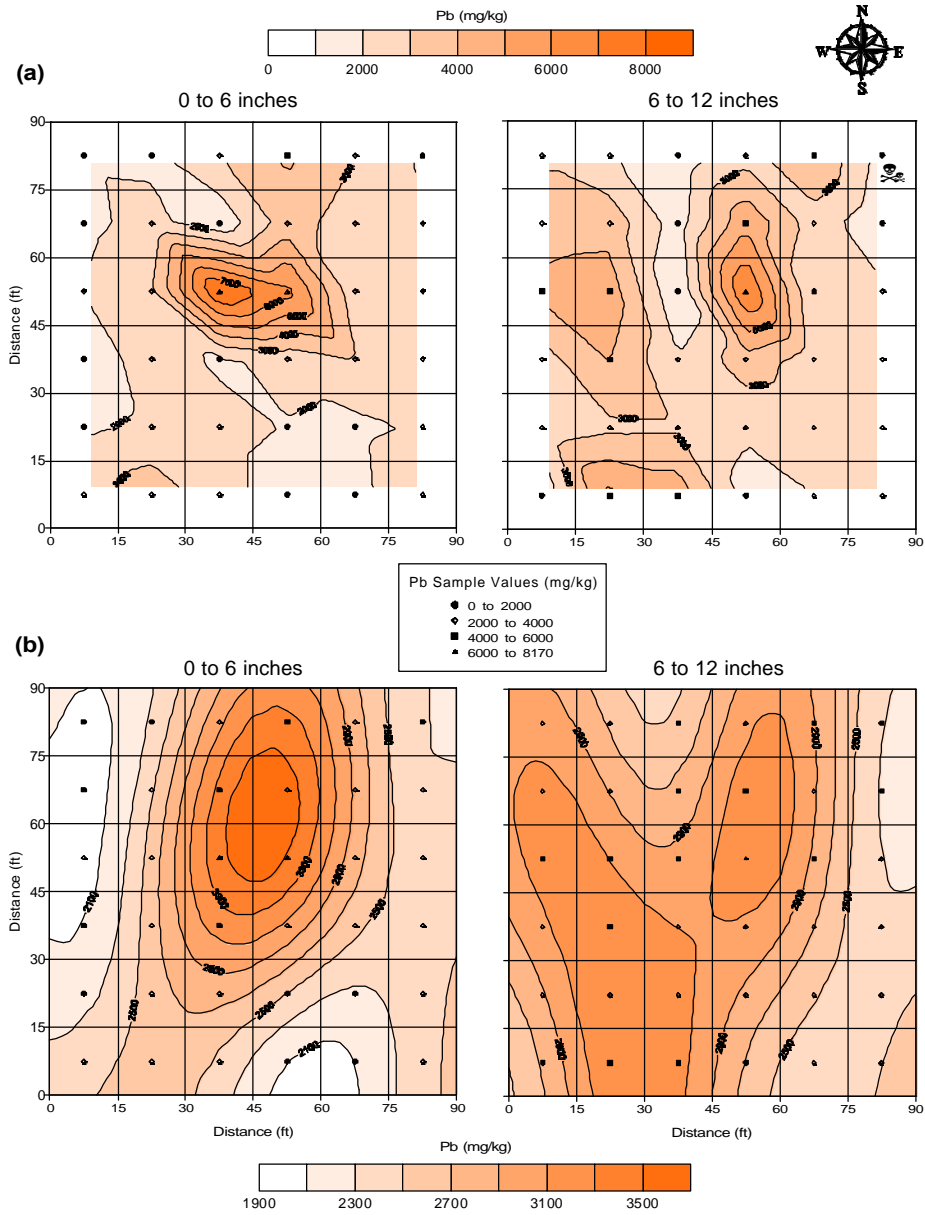


Figure 3
Maps of Site C Initial Soil Lead Based on
(a) Triangulation with Linear Interpolation and (b) Kriging Interpolation

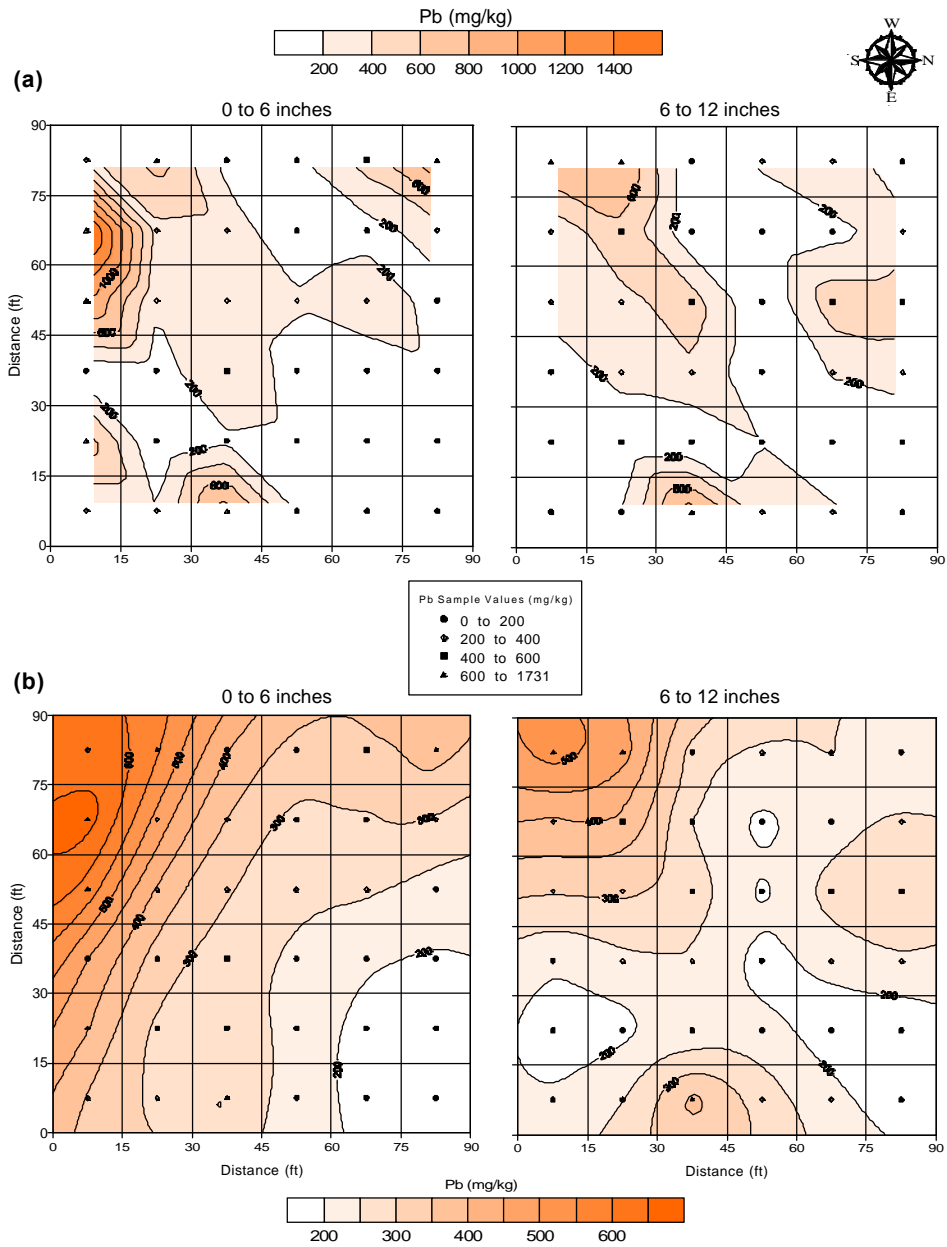


Figure 5
Maps of Site 129-3 Initial Soil Lead Based on
(a) Triangulation with Linear Interpolation and (b) Kriging Interpolation

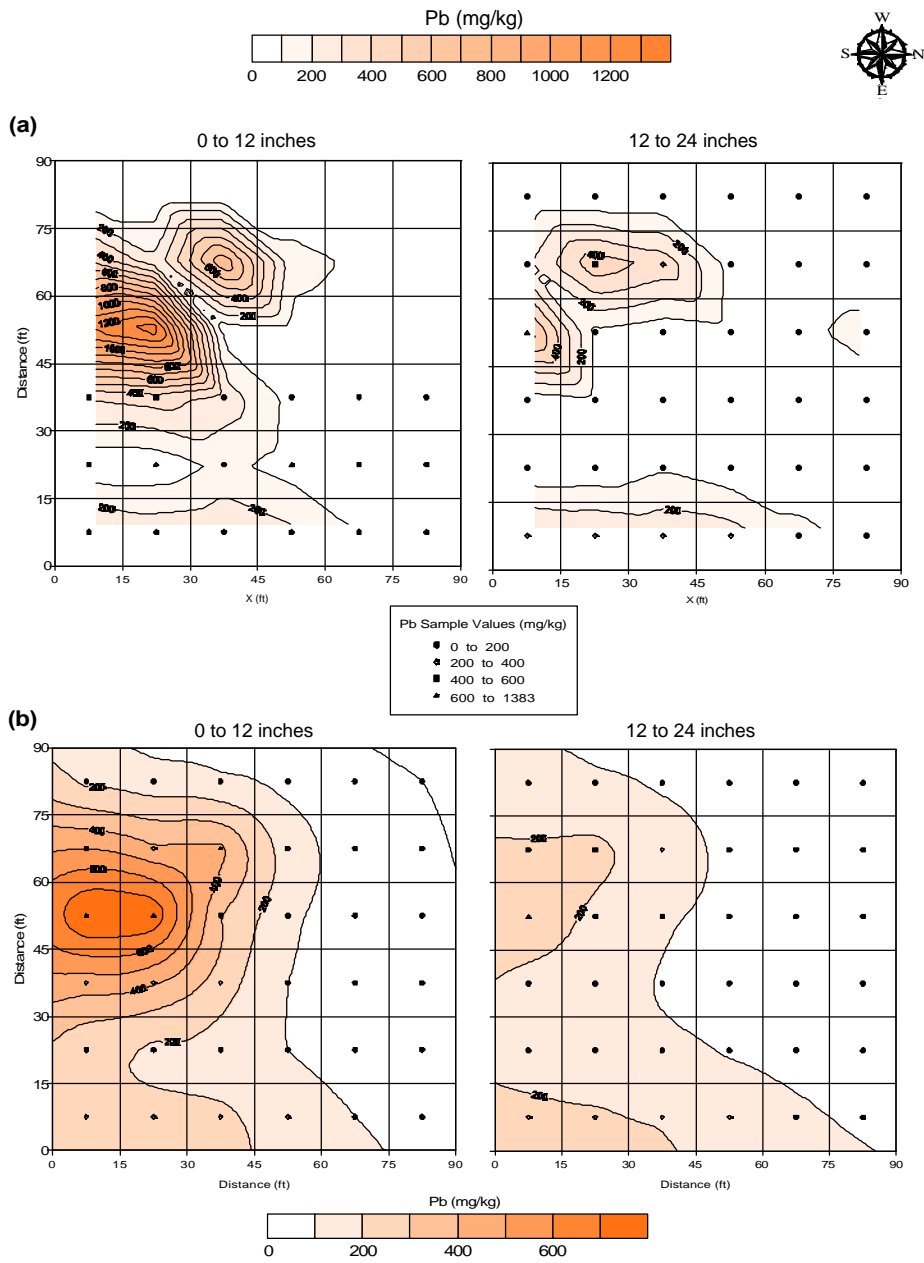


Figure 6
Maps of Site 129-3 Post-Mustard Soil Lead Based on
(a) Triangulation with Linear Interpolation and (b) Kriging Interpolation

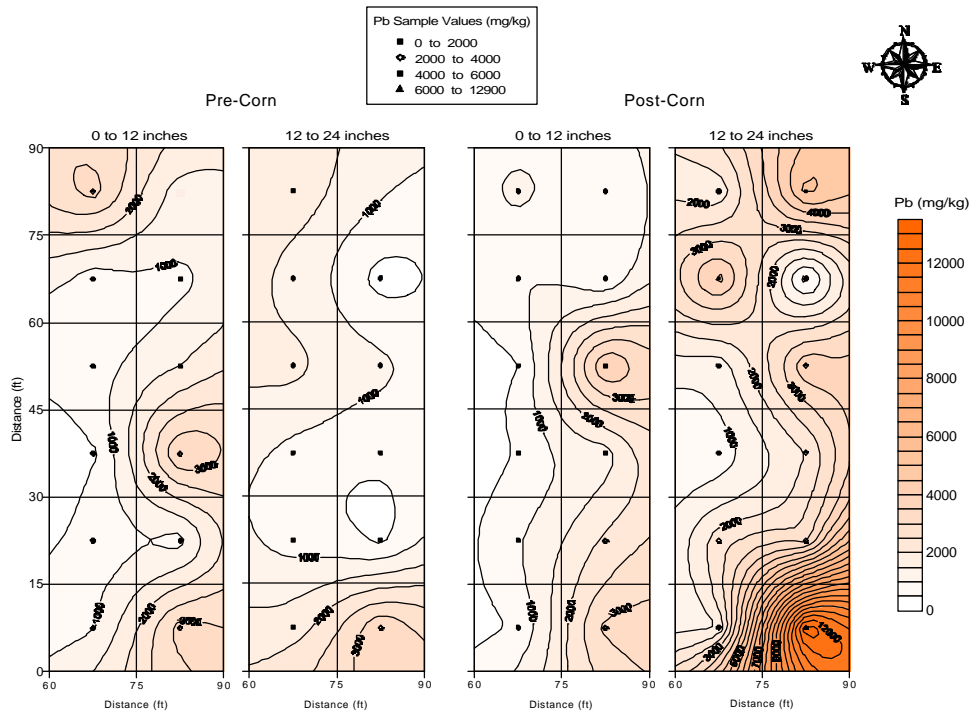


Figure7
Maps (Kriging Interpolation) of Site C, Pre- and Post-Corn,
from 1999 Results for Total Lead in Soil

The above plots are for the 1999 total lead in soil at Site C specified by time interval and sampling depth. The sampling event for 1999 Site C was limited to the eastern 1/3 of the site due to poor crop growth. The very high value of 12,900 mg/kg observed at the southeastern corner of the site is an anomaly most likely due to particulate lead in the soil.

References:

Abramowitz, M., and I. Stegun, (1972), Handbook of Mathematical Functions, Dover Publications, New York.

Cressie, N. A. C. (1991), Statistics for Spatial Data, John Wiley and Sons, Inc., New York, 900 pp.

Golden Software, Inc., "Surfer 7 Users Guide," Golden Software, Inc., Golden, Colorado, 1999.

Guibas, L., and J. Stolfi (1985), "Primitives for the Manipulation of General Subdivisions and the Computation of Voronoi Diagrams," ACM Transactions on Graphics, 4(2):74-123.

Journel, A.G., and C. Huijbregts, (1978), Mining Geostatistics, Academic Press, 600 pp.

Lawson, C. L. (1977), "Software for C1 Surface Interpolation," in Mathematical Software III, J. Rice (ed.), Academic Press, New York, pp. 161-193.

Lee, D. T., and B. J. Schachter, (1980), "Two Algorithms for Constructing a Delaunay Triangulation," International Journal of Computer and Information Sciences, 9(3):219-242.